

Influence of the synthesis conditions and growth environment on MFI zeolite film orientation

Sau Man Lai, Louisa Tak Yin Au, King Lun Yeung^{*}

Department of Chemical Engineering, Hong Kong University of Science and Technology, Clear Water Bay, Kowloon, Hong Kong, PR China

Received 7 August 2001; received in revised form 26 February 2002; accepted 4 March 2002

Abstract

Zeolite powders and films were prepared from six published synthesis recipes claimed to produce zeolite film coatings and membranes with (200), (020), (002) and (101) orientations. The morphology and orientation of the zeolite films prepared from each synthesis recipe were characterized and compared to determine the influence of synthesis composition and crystallization conditions. The zeolite growth environment was manipulated by changing the seed concentration on the substrate. The experimental results indicate that the synthesis chemistry and crystallization conditions affect the crystal grain morphology, whereas the growth environment influences the crystal habit. A simple method for predicting the orientation of the zeolite film based on the morphology of the zeolite crystal and the growth environment is also presented. © 2002 Elsevier Science Inc. All rights reserved.

Keywords: Zeolite preparation; Sil-1; Boron-silicalite-1; MFI zeolite film; Film orientation; Grain morphology

1. Introduction

The synthesis composition, crystallization conditions and growth environment are known to affect the shape of the zeolite crystals. This is particularly true for zeolites that display anisotropic growth behavior, such as zeolite MFI [1]. The recent work of Iwasaki et al. [2] clearly demonstrates that the growth rate and crystal morphology of silicalite-1 (Sil-1) powder are strongly affected by the composition of the synthesis mixture. Earlier work of Hayhurst [3] shows that decreasing the alkalinity of the hydrogel results in a

significant elongation of the prismatic Sil-1 crystals. Besides the well-known prismatic crystals, MFI zeolites have been synthesized with different shapes. Twinned crystals are common [4,5], while near-spherical zeolites can be obtained when potassium and boron are added [6–8]. Cubic and rectangular crystals with rounded ends are prepared from concentrated solutions and dense gels [7,9], whereas cesium ZSM-5 has a plain rectangular shape [10]. Use of the bi-quarternary ammonium ion gave leaf-shaped ZSM-5 crystals [11].

The individual crystallographic planes of MFI crystals possess different activation energies that are strongly dependent on the synthesis composition [12–16]. This means that zeolite MFI is especially sensitive to the perturbations in the local nutrient concentration. The growth environment

^{*} Corresponding author. Tel.: +852-2358-7123; fax: +852-2358-0054.

E-mail address: kekyeung@ust.hk (K.L. Yeung).

plays an important role in the zeolite growth [7,17,18]. It can have significant effects on the crystallization rate, size distribution and crystal morphology. Gabelica and Derouane [17] suggest that viscous synthesis solutions can impede the dissolution-growth competitive process resulting in a faster zeolite growth rate. The zeolites formed from a clear solution, a dispersed low-density gel, a separated high-density gel and a solid phase have different shapes [18]. Pyramidal, conical, trapezoidal and cubic crystals are some of the shapes observed when ZSM-5 is crystallized from dense gel spheres [7]. The malleability of the zeolite crystal shape is an important attribute that enables the engineering of zeolite film and membrane microstructures for various applications [19–23].

Zeolite coatings are in general prepared either by a direct one-step synthesis using the in situ method or by the pre-seeding and regrowth procedure (i.e. ex situ method). The former method has been described by Suzuki [24], Haag and Tsikoyiannis [25,26], Jansen et al. [27] and Geuss et al. [28] for the preparation of membranes and catalytic coatings. Haag and Tsikoyiannis [25] are among the pioneers in zeolite membrane research. Using non-silicious solid surfaces (e.g. Teflon, silver, stainless steel) as substrates, they prepared continuous layers of polycrystalline ZSM-5 films. Noack et al. [29] have demonstrated that a silicalite-1 film with a preferred orientation can also be prepared by a one-step crystallization. In situ crystallization (i.e. seed-free) of MFI zeolites onto silicon wafer [30] and quartz disks [31] usually yields films with $\langle 020 \rangle$ or $\langle 200 \rangle$ out-of-plane orientations. In the ex situ synthesis technique, the support is pre-seeded with zeolite crystals.

Both crushed zeolite powders [32] and colloidal zeolite sols [33] have been successfully used as seeds in membrane preparation. These seeds have been rubbed onto the support, applied as a paste, slip-casted and even spin-coated to form a uniform seed layer [32–35]. Seeds have also been chemically grafted onto the support [36]. Xomeritakis et al. [37] reported that the growth mechanism and final film microstructure are affected by the presence of the seed layer and by the synthesis conditions. Zeolite membranes grown onto seeded supports from dilute synthesis solutions usually display a

$\langle 101 \rangle$ out-of-plane orientation, but at a higher crystallization temperature (448 K), the zeolites are oriented with their *c*-axis normal to the seed layer [37,38]. Hedlund et al. [39] have prepared thin silicalite-1 films on silicon wafers pre-coated with a layer of seeds. They reported that the zeolite film orientation changes with the seed size and coverage.

Moreover, the incorporation of silicate species onto the growing MFI crystal plane is intrinsically anisotropic [14] leading to a preferred growth orientation of the crystal grains. A number of mechanisms have been proposed for the growth of zeolite films with preferred orientation. One mechanism is that the preferred orientation develops from randomly oriented seeds because of the anisotropic growth rates of the zeolite [39]. This mechanism is well known in crystallography and geology where models for predicting a preferred orientation from growth anisotropy have been developed. Among these models is the van der Drifts growth model [40] that predicts a columnar growth for MFI zeolite. More recently, the growth of 002-oriented MFI zeolites on uniformly seeded supports has been modeled by Bonilla and coworkers [41]. This paper attempts to rationalize the formation of different MFI zeolite film microstructures and orientations from various synthesis recipes reported in the literature. The purpose is to create a simple guiding principle for the synthesis of zeolite coatings with the desired layer microstructure and crystallographic orientation. The growths of free-floating silicalite-1 crystals and silicon (100)-supported silicalite-1 films under synthesis conditions known to give zeolite films with preferred (101), (002) and (200)-orientations are investigated. In addition, the influence of the growth environment (i.e. 3D versus 2D) and seed concentration on the film microstructure and orientation is examined in detail.

2. Experimental

2.1. Preparation of Sil-1 seeds, crystals and films

Colloidal TPA-silicalite-1 seeds were prepared from a synthesis solution with the composition

10SiO₂:2.5TPAOH:0.8NaOH:110H₂O. 0.85 g of sodium hydroxide were added to 60 cm³ of a 1 M tetrapropylammonium hydroxide (TPAOH) solution. 15 g of fumed silica were added to this solution. The mixture was vigorously stirred at 353 K until a clear, homogeneous solution was obtained. The resulting solution was transferred into a 125 cm³ Teflon bomb and aged for 24 h at room temperature. The Teflon container was then inserted into a stainless steel autoclave (home-made) and heated in an oven (Memmert) at 398 K for 8 h. The resulting product was repeatedly rinsed with deionized, distilled (DDI) water and centrifuged until it reached a pH value below 10. A 4 wt.% colloidal suspension of TPA-Sil-1 seeds (~120 nm ellipsoidal crystallites) was obtained by dilution. The zeolite sol was stable and remained in suspension even after 6 months of storage.

TPA-silicalite-1 powders were prepared from the list of synthesis compositions and crystallization conditions shown in Table 1. In a typical solution (e.g., recipes 1 and 2), tetraethyl orthosilicate (TEOS) was added drop-by-drop to an alkaline solution containing TPA⁺ and OH⁻ ions as well as other additives such as boric acid. After aging the solution overnight to ensure complete hydrolysis of the silicate, 2.5 mg of zeolite seeds were added to serve as nucleation centers for the growth of zeolite crystals. Zeolite crystallization was allowed to proceed in an oven set at the desired temperature for different lengths of time. After the hydrothermal treatment, the zeolite crystals were separated from the mother liquor using a centrifuge (Heraeus Sepatech) at a speed of 12,000 rpm for 40 min. The supernatant was carefully de-

canted and the residue was rinsed with DDI water. The pH value of the rinsed solution was measured with a calibrated pH meter (Schott Geräte). This procedure was repeated 3–4 times until the pH value of the rinsed solution was below 10. This ensured the removal of unreacted silica and organic template. A portion of the recovered powder was dried in an oven ($T = 393$ K) and kept for later analysis.

Silicalite-1 films were deposited onto single crystal Si(100) wafers using the synthesis recipes listed in Table 1. The silicon wafer was rinsed with DDI water and ethanol, blown-dried with compressed air to remove water stains and then dried in an oven at 333 K. The silicon was pre-seeded with colloidal TPA-Sil-1 zeolites. The seed were chemically grafted onto the silicon using mercapto propyltrimethoxysilane. The seed population was varied from 0 (unseeded substrates) to 95 seeds/ μm^2 for a fully seeded surface. The seeded substrates were dried in air at room temperature for 6 h, followed by oven drying overnight at 333 K before calcination in air (i.e. $T = 823$ K, $t = 6$ h). The silicon substrates were placed on a Teflon holder that positions the wafers horizontally at a fixed height with the seeded surface facing downward. The wafers and the holder were placed in the Teflon autoclave vessel to which the synthesis solution was added. The volume of solution was calculated to give a roughly similar volume-to-seed ratio as that used in the powder synthesis. The level of the solution was usually between 5 and 10 mm above the wafers. Crystallization was conducted in a pre-heated oven for the desired length of time. The samples were recovered, rinsed, dried

Table 1
Composition of the synthesis solutions and crystallization conditions employed in this study

Recipe	Synthesis composition	Reaction temperature (K)/ time (h)	Film orientation	Reference
1	40SiO ₂ :9TPAOH:9500H ₂ O:160EtOH	413/4–20	(101)	[37]
2	40SiO ₂ :9TPAOH:9500H ₂ O:160EtOH	448/4–20	(002)	[37]
3	10SiO ₂ :0.22Na ₂ O:0.52TPABr:200H ₂ O	362/36–216	(011)	[42]
4	25SiO ₂ :3TPAOH:1500H ₂ O:100EtOH	373/120 (in oil bath)	(100)	[39]
5	K-synthesis	413/16	(100)	[42]
6	40SiO ₂ :10TPAOH:40boric acid:20,000H ₂ O: 160EtOH	403/48–192	–	–

and calcined to produce the Si1-1/Si(100) films examined in this study.

2.2. Sample analysis and characterization

A Philips PW1830 X-ray diffractometer was employed for identifying the zeolite type, crystallinity and texture of the zeolite powder and film samples. Using a $\text{CuK}\alpha$ radiation source ($\lambda = 0.1508$ nm), data were taken between $5^\circ \leq 2\theta \leq 45^\circ$ at a scanning rate of $0.02^\circ/\text{s}$. The morphology of the zeolite crystals and films was examined by scanning electron microscopy (JEOL 6340F and JEOL 6300). The powder samples were prepared by depositing a few drops of the washed solution (dispersed in ethanol) onto an aluminum specimen holder where it was allowed to dry. The sample were analyzed without coating using a JEOL 6340F microscope operating in the SEM mode at 2 kV (emission = $12 \mu\text{A}$). The zeolite/Si samples were mounted on aluminum stubs using conducting adhesive and coated with a layer of gold (~ 300 Å) using a sputter coating machine (Denton Model Desk II) and imaged by the scanning electron microscope (SEM JEOL 6300) operated in the SEM mode at 15 kV. The SEM pictures were obtained in digital form and analyzed by an image analysis software (Leica).

2.3. Materials

The chemicals used in the zeolite powder and film synthesis were fumed silica (Aerosil 200), colloidal silica (Ludox HS-40), tetraethyl orthosilicate (98 wt.%, Aldrich), tetrapropylammonium bromide (>98 wt.%, Fluka), tetrapropylammonium hydroxide (1 M, Aldrich), sodium hydroxide (98 wt.%, Baker), boric acid (99 wt.%, Sigma) and DDI water. Silicon wafers (100) were purchased from JXC Polished Wafers. The hydrothermal treatments were carried out in home-made Teflon-lined stainless steel autoclaves (125 cm^3). After the synthesis, the autoclaves and Teflon bombs were cleaned using KOH solution (4 M) under hydrothermal conditions ($T = 393$) for 24 h to remove any zeolite crystals that may have deposited on the wall of the vessel.

3. Results and discussion

3.1. Zeolite powder synthesis

Table 1 lists the synthesis compositions and preparation procedures used by different authors to obtain zeolite films and membranes with preferred crystallographic orientations [37,39,42]. Using identical synthesis recipes, zeolite powders were prepared and analyzed in order to study the effects of the synthesis conditions on the zeolite morphology. The size and dimensions of the zeolite powders were based on 50 direct measurements from a series of SEM pictures of the sample.

3.1.1. Dilute synthesis solution

MFI zeolite membranes with preferred (101) and (002)-crystallographic orientations [37] have been successfully prepared from dilute synthesis mixtures containing silica, TPA^+ and OH^- on seeded supports at low (i.e. <413 K) and high (i.e. $433 < T < 473$ K) temperatures, respectively. Fig. 1a displays the growth behavior of zeolite powders prepared from recipe 1 using 2.5 mg/l of zeolite seeds (Table 1). It is clear from the figure that the zeolite growth is anisotropic with the growth rate along the crystal length (l) being the fastest followed by the width (w) and the depth (d). All three dimensions show a monotonic increase with time. During the 20 h of crystallization, the length-to-width ratio of the zeolite crystals varies from 1.3 to 1.6. The prismatic shape of the zeolite crystal is not well developed at the early stage of crystallization, and a significant amount of twinned crystals is present in all samples. The (101) crystallographic planes are only apparent after prolonged synthesis as shown in the inset of Fig. 1a. Zeolites prepared at higher temperature (recipe 2) display little variation in their length-to-width ratio (i.e. ~ 1.8) as crystallization progresses (Fig. 1b). Prismatic and twinned crystals are present in equal abundance. As in the case of the low-temperature synthesis, a monotonic increase in crystal size was observed. Despite the difference in the synthesis temperatures, the zeolites made from the two batches do not exhibit a significant difference in their general morphology (Fig. 1b, inset).

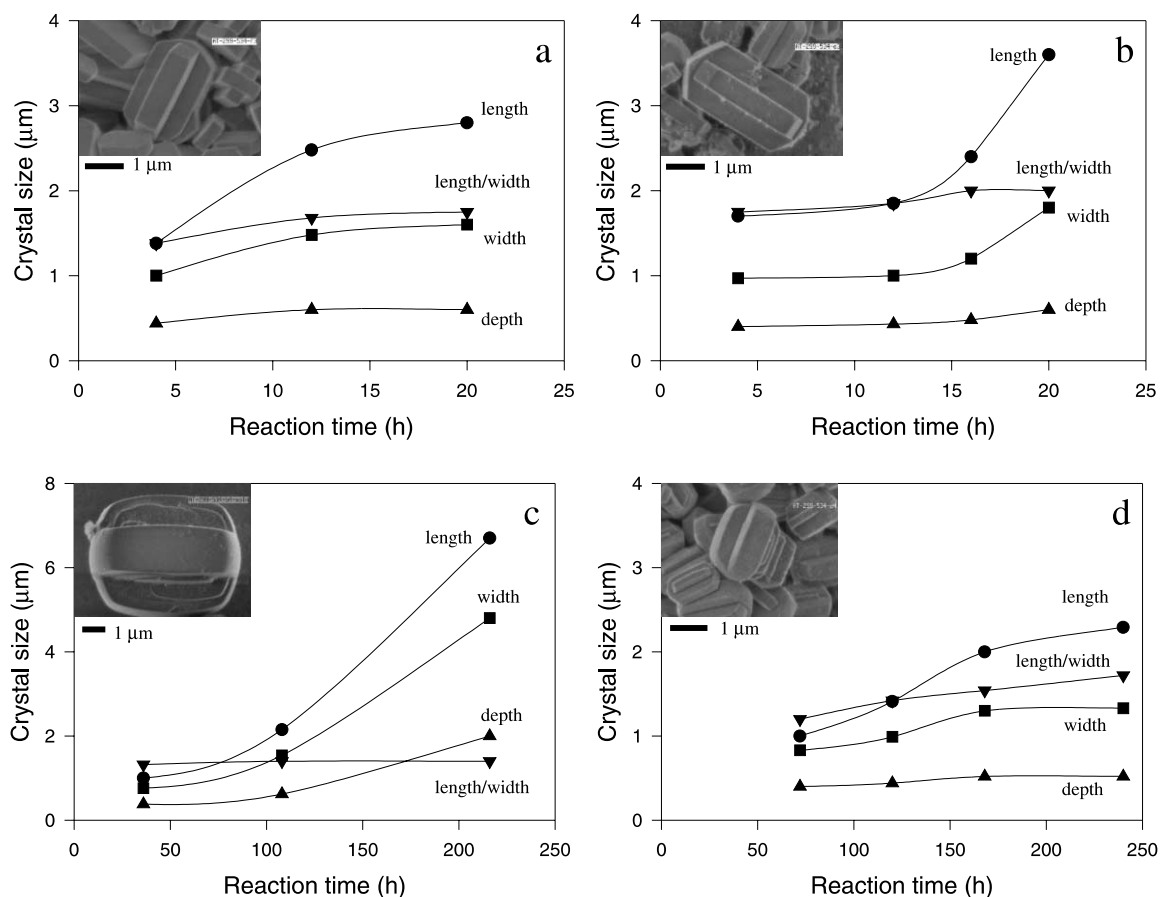


Fig. 1. Crystal size (width, length and depth) and length/width ratio as a function of crystallization time for zeolite powders prepared from (a) recipe 1 (40SiO₂:9TPAOH:9500H₂O:160EtOH at 413 K), (b) recipe 2 (40SiO₂:9 TPAOH:9500H₂O:160EtOH at 448 K), insets: SEM micrograph of the zeolite powder after 20 h of crystallization. (c) Recipe 3 (10SiO₂:0.22Na₂O:0.52TPABr:200H₂O at 363 K), inset: SEM micrograph of the zeolite powder after 216 h of crystallization, (d) recipe 4 (25SiO₂:3TPAOH:1500H₂O:100EtOH at 373 K), inset: SEM micrograph of the zeolite powder after 10 days of crystallization.

3.1.2. Concentrated synthesis solution

MFI zeolite membranes with a (101)-orientation have also been obtained from concentrated synthesis solution (recipe 3) as reported in the patent literature [42]. Although this synthesis solution contained a high silica concentration, it remained clear and homogeneous with no apparent gel formation. The seed concentration was fixed constant at 2.5 mg/l. Fig. 1c also shows a monotonic increase in the length (l), width (w) and depth (d) of the zeolite particles as a function of synthesis time. The length-to-width ratio of the particles remained constant at a value of 1.4 during the

synthesis. The crystal sizes (measured from the diagonals of the *mother* crystals) increases with synthesis time from 0.5 μm to more than 6 μm during the 220 h synthesis. Amorphous material was present on the zeolites particles prepared at short synthesis time. Most of the zeolites are twinned and resemble the crystals prepared from the dilute synthesis solutions (Fig. 1c, inset).

3.1.3. ($h00$) synthesis solutions

MFI zeolite membranes with ($h00$)-preferred crystallographic orientations have been prepared by reflux at ambient pressure (recipe 4), with the

addition of potassium (recipe 5) and by the incorporation of boron (recipe 6). The zeolite powder prepared by the reflux method is a mixture of prismatic and twinned crystals (Fig. 1d). SEM analysis indicates an elongation in the shape of the zeolite crystals with synthesis time, and is shown by the monotonic increase in the length-to-width ratio as a function of time. The crystal size as measured from the length, width and depth of the individual zeolites displays a monotonic increase with time. There is a similarity between the shape of the zeolite powder from this batch to those prepared by recipes 1, 2 and 3 (Fig. 1d, inset).

Fig. 2 shows the effects of potassium on zeolite crystal growth and morphology. A different crystal morphology was obtained from this set of syn-

thesis (i.e. recipe 5). SEM images of the recovered products show spherical particles at the early stages of zeolite synthesis (Fig. 2a). It is probable that they are gel-spheres formed from the reactions between the silica and the templating agent. There is evidence that the zeolite crystals were embedded between these substances. Twinned and intergrown crystals were frequently observed at longer synthesis time (Fig. 2b). In most cases, instead of growing out perpendicularly from the (010) crystal plane, the intergrowth formed a “cross” with the mother crystal (Fig. 2b). Also, the appearance of ridges is common on the surfaces of these zeolite crystals (Fig. 2c). The crystal size increased from 0.7 to 6 μm during the 16 h of synthesis, and the crystals retained their near-spherical shape. In-

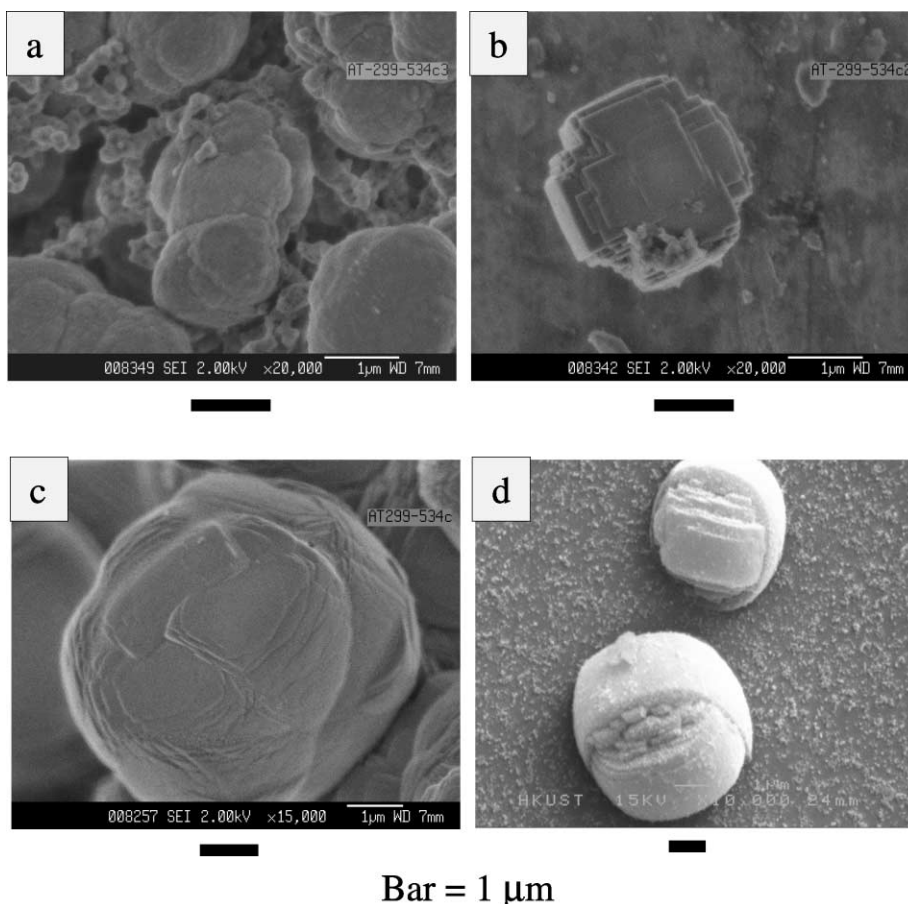


Fig. 2. SEM images of zeolite crystal particles grown from K-synthesis solution at 413 K for (a) 8, (b) 12 and (c) 16 h, (d) SEM picture of a zeolite grown from boron-containing synthesis solution.

corporation of boron into zeolite MFI was reported to produce heavily twinned, near-spherical zeolites with a morphology similar to that of KZSM-5. This was indeed the case as seen from a comparison of the zeolites prepared from the boron-containing recipe 6 (Fig. 2d) with the crystals prepared from recipe 5 (Fig. 2c). Whereas boron is inserted into the MFI zeolite framework, potassium is present as an ion-exchangeable counterion within the zeolite cages.

It can be seen that there is no significant difference in the shape of the zeolite crystals prepared from synthesis recipes that are reported to grow zeolite layers with preferred crystallographic orientations of (101) (i.e. recipes 1 and 3), (002) (i.e. recipe 2) and (100) (i.e. recipe 4). Except for the more rounded edges of the zeolites obtained from recipes 3 and 4 (i.e. orthorhombic crystals), the four synthesis recipes gave identical crystal morphologies. They displayed both prismatic and twinned crystals that have a length-to-width ratio of 1.4 to 1.8 (cf. Fig. 1). Although the zeolite growth rates are different because of the differences in synthesis composition, chemical precursors and crystallization temperature, the growth along the *c*-axis (i.e. length) is consistently faster than that along the other two axes. According to van der Drift's growth model [40], only the grains oriented with their fastest growing direction perpendicular to the substrate and pointing towards the nutrient survive the intense competition from its neighbor. Thus, the zeolite films prepared from recipes 1–4 should all exhibit an identical (002) crystallographically preferred orientation. The model also proved inadequate in describing the formation of identical film orientations from synthesis recipes (i.e. recipes 4–6) that yield morphologically dissimilar crystals (Figs. 1d and 2). It is clear that the final membrane morphology is not dictated solely by the growth kinetics (i.e. van der Drift's growth model), but is also influenced by the immediate growth environment.

3.2. Relationship between zeolite growth environment and film orientation

The growth environment of the free-floating zeolite crystals is different from that of the zeolites

growing within the confines of a film. In the former case, the suspended zeolites are growing within a uniform concentration field (Fig. 3a), whereas the supported zeolite grains due to the constraint of a 2D geometry experience a non-uniform concentration field as illustrated in Fig. 3b. Under most circumstances, the growth of the zeolite *into* the support is negligible and the crystal grains tend to grow outward towards the synthesis solution. This and the growth competition between neighboring grains dictate the morphology and habit of the individual grains and help shape the overall film microstructure and orientation. In order to investigate the role of growth environment on the film orientation, a series of silicalite-1 films were grown from synthesis recipes 1, 2 and 6 that were reported to form (101), (002) and (200)-oriented zeolite films on seeded supports [37,43]. A Si(100) single crystal wafer was chosen as substrate to prevent the introduction of foreign ions (e.g. Al³⁺). The wafers were polished to less than 10 nm roughness, and were uniformly seeded with Sil-1 nanocrystals (~120 nm) to give seed populations between 0 and 95 seeds per μm^2 . It is important to note that the seed population is the average number of *exposed* seeds that occupy a $100\ \mu\text{m} \times 100\ \mu\text{m}$ area. More than one measurement was obtained for each seed population. In addition, the average growth rate along the *c*-axis of the crystal grains was measured from the SEM micrographs. More than 100 measurements constitute each rate data and in some cases about 500 measurements were made.

3.2.1. (101) synthesis solution (recipe 1)

Fig. 4 displays the surface morphology of Sil-1 films grown on silicon wafers with different initial seed concentrations. The films were crystallized from the same synthesis solution. It can be seen from the SEM figures that the seed population has a direct impact on the membrane microstructure. It was found that about 5×10^{-3} seeds/ μm^2 were nucleated onto the unseeded silicon wafer during the synthesis, which served as growth centers for zeolite crystallization. At this seed concentration, the distance between neighboring seeds was more than 10 μm . This means that the concentration of nutrient immediately surrounding the seeds can be

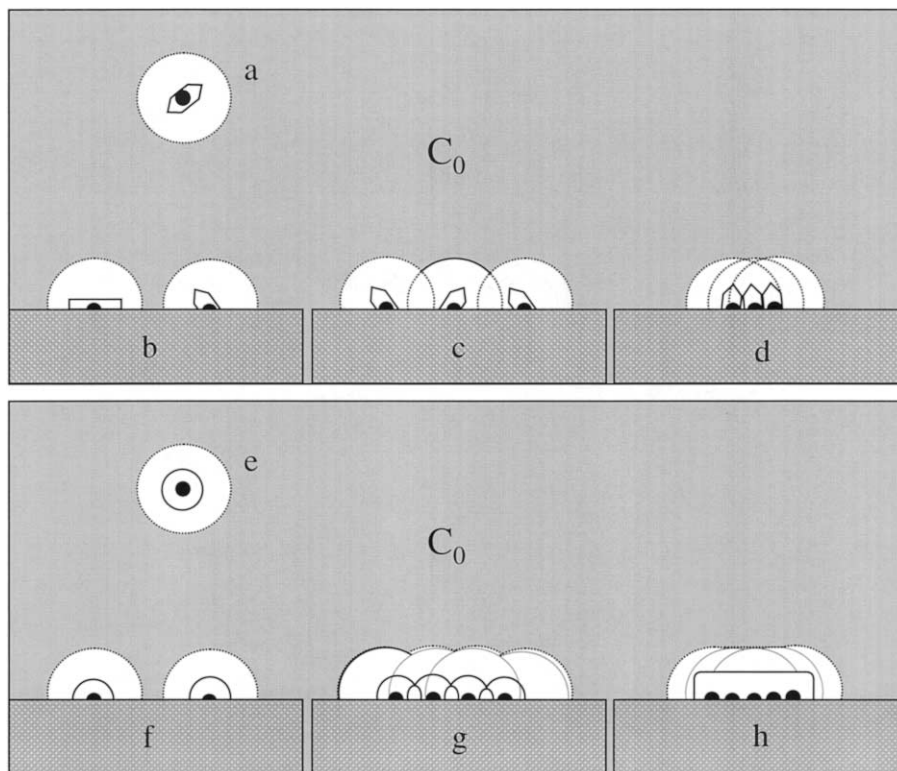


Fig. 3. Schematic diagram of zeolite growth in solution and on a seeded flat support. Anisotropic zeolite crystals growing from (a) seeds floating in solution and on a (b) sparsely, (c) moderately and (d) densely seeded support. Isotropic zeolite crystals growing from (e) seeds floating in solution and on a (f) sparsely, (g) moderately and (h) densely seeded support. (C_0 is the bulk concentration of the nutrient).

regarded as “uniform” (i.e. Fig. 3b) and the growing crystals should not exhibit any preferred habit. Indeed, off-plane crystal growth was observed in the SEM images, but was not as common as the in-plane zeolite growth (Fig. 4a). The latter zeolites were oriented with their (020) facet plane parallel to the surface (Fig. 4a, inset). The morphology of the flat crystals paving the surface of the silicon is similar to that of the powder (Fig. 1a). Although the growth is confined to 2D, the time series study indicated that like the powder synthesis the growth along the c -axis is still the fastest (i.e. $0.4 \mu\text{m/h}$) and the film orientation is due mainly to the crystal habit. In fact, the growth along the film thickness (i.e. (020)) is still the slowest at $0.1 \mu\text{m/h}$. Some of these zeolites display secondary crystal growth on their (020) facet. The secondary crystals are mostly oriented with their b -

axis normal to the substrate as shown in the SEM figures. Indeed, XRD analysis of the sample (Fig. 5a) indicates that the deposited zeolite layer has a preferred orientation of (200/020). It had been argued that the flat crystal is the preferred habit of the MFI zeolites on the support since it is the most stable configuration [30].

Seeding the support introduces more growth centers resulting in greater competition for nutrient and space. This also causes perturbation in the local nutrient concentration (Fig. 3c) that can have a large impact on the zeolite growth. Fig. 4b shows a silicalite-1 film grown on a uniformly seeded silicon wafer containing five seeds/ μm^2 (i.e. 5% surface coverage). The film exhibits a greater number of off-plane growths. These zeolite crystals grew at an angle away from the substrate, mostly between $25\text{--}75^\circ$ (Fig. 3b, inset). However, the

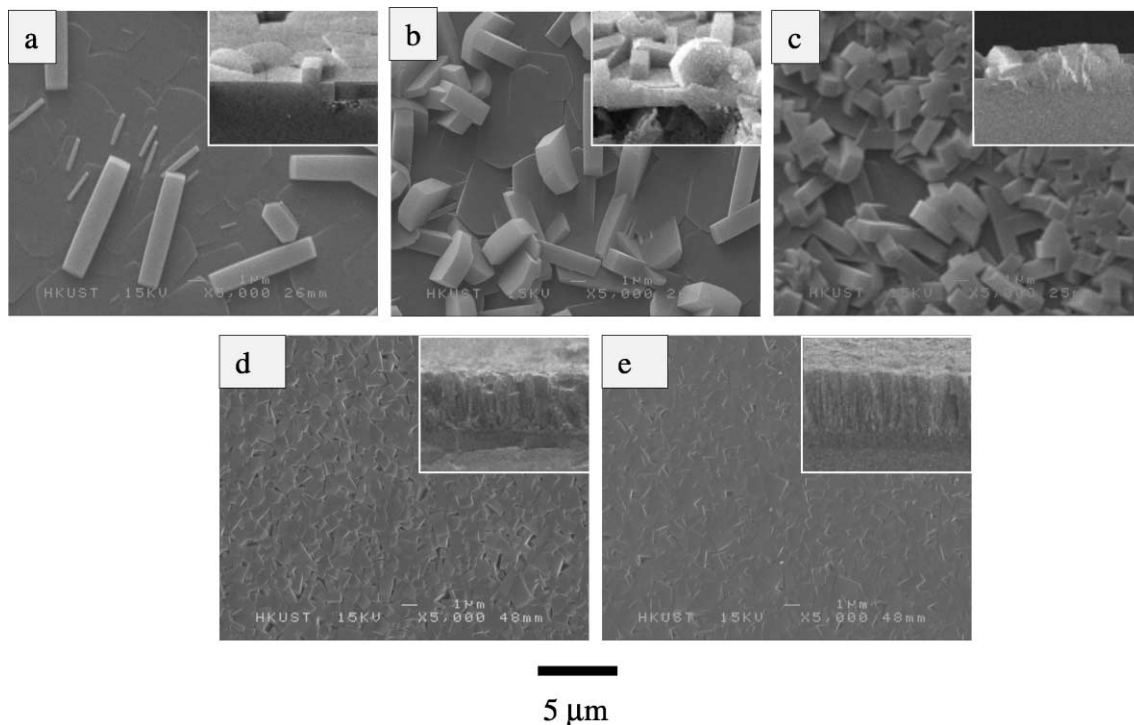


Fig. 4. SEM images of zeolite films grown from the synthesis solution containing $40\text{SiO}_2:9\text{TPAOH}:9500\text{H}_2\text{O}:160\text{EtOH}$ at 413 K for 20h on silicon pre-seeded with (a) 0, (b) 5, (c) 7.3, (d) 29 and (e) 95 seeds/ μm^2 .

XRD pattern displays mainly diffraction peaks corresponding to $(h00)$ and $(0k0)$ planes as shown in Fig. 5b. The number of off-plane zeolite crystals is significantly larger for the Sil-1 film grown on silicon with 0.08 monolayers of seeds or 7.3 seeds/ μm^2 (Fig. 4c), and the X-ray diffraction peak corresponding to (101) is evident in the sample (Fig. 5c). Zeolite grains that grew with their c -axis tilted away from the substrate are more common after seeding, but they are also found in films grown on unseeded silicon (Fig. 4a). These zeolites appear as truncated crystals growing out of the support (Fig. 4b–c) and both prismatic (i.e. with rounded ends) and twinned morphologies have been observed. These crystals have an average growth rate along the c -axis of 0.24 $\mu\text{m}/\text{h}$ or roughly half that observed in (020) -oriented grains (cf. Fig. 4a). This may be due to the fact that unlike the flat crystal grains, the zeolite growth in these crystals occurs only in one direction along the c -axis (i.e. outward).

As the seed population was further increased (i.e. 29 seeds/ μm^2 or 0.3 ML), there is a significant improvement in crystal intergrowth (Fig. 4d) but due to growth competition, the grain size is smaller. From the cross-section (Fig. 4d, inset) it can be seen that the zeolite crystals are aligned nearly vertically on the support. The XRD pattern shown in Fig. 5e indicates that the film has a (101) orientation. Fig. 4e displays the zeolite film obtained from a seed population of 95 seeds/ μm^2 (i.e. corresponding to a complete surface coverage). The intergrowth between neighboring crystals is excellent as shown in this figure, but the grain size is small. From both the film cross-section (Fig. 4e inset) and the XRD data (Fig. 5f), it can be seen that the film has a (101) -crystallographically preferred orientation. A change in crystal morphology is observed at high seed concentration. Instead of truncated crystals, the grains can be described as inverted pyramids with a rectangular base. This is mainly due to the growth of zeolites from

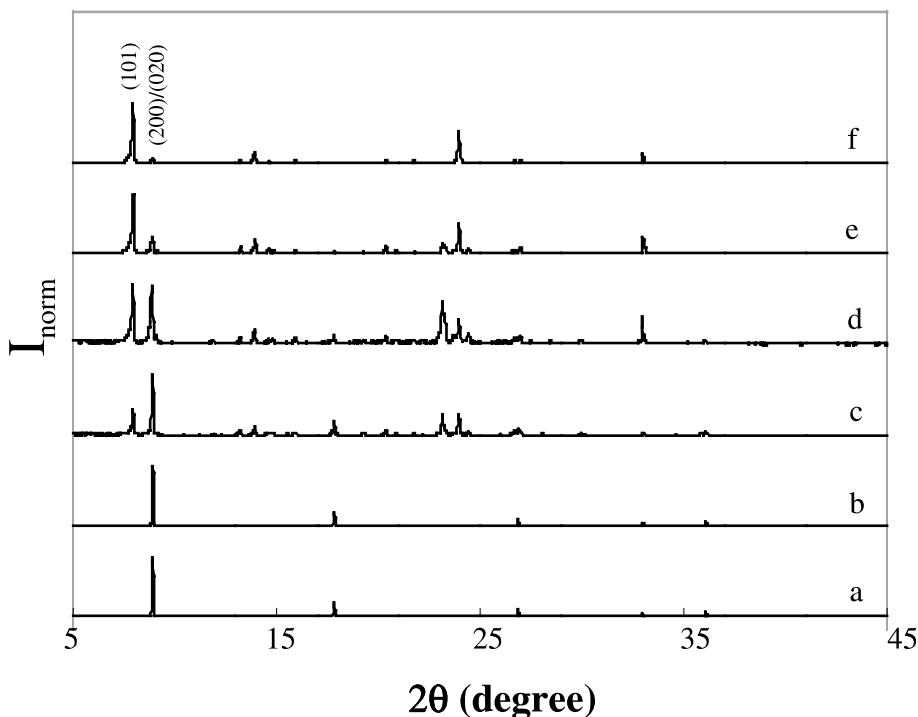


Fig. 5. XRD patterns of silicalite-1 films grown from synthesis solution containing 40SiO₂:9TPAOH:9500H₂O:160EtOH at 413 K for 20 h on silicon pre-seeded with (a) 0, (b) 5, (c) 7.3, (d) 13, (e) 29 and (f) 95 seeds/ μm^2 .

sub-micrometer seeds to multi-micrometer sized grains in such a confined environment (Fig. 3e). The growth rate along the length of these pyramidal crystals (Fig. 4d and e) was measured to be 0.15 $\mu\text{m}/\text{h}$, or about 0.22 $\mu\text{m}/\text{h}$ along the *c*-axis. It is clear from Figs. 4 and 5 that both the film morphology and orientation change with the initial seed population.

3.2.2. (002) synthesis solution (recipe 2)

Shown in Fig. 6 are the microstructures of Sil-1 films grown on silicon wafers with seed populations of 0, 7.5, 30 and 95 seeds/ μm^2 using the synthesis composition and procedure outlined for recipe 2. The unseeded silicon substrate was grown over by a layer of flat crystals that have the characteristic shape of zeolite MFI (Fig. 6a). Similar to its powder counterpart (Fig. 1b, inset), the crystal grains are prismatic in shape with well-developed (101) facets. As in the case of the powder, the growth along the *c*-axis of the zeolite grain is the

fastest (0.45 $\mu\text{m}/\text{h}$). Although the X-ray diffraction pattern of the film indicates a preferred (020) orientation along the thickness, the grains are in fact randomly arranged within the layer as shown in Fig. 6a. Presence of a (200) secondary crystal growth is also evident in the SEM image. A significant increase in off-plane zeolite growth was observed after introducing small quantities of seeds (7.5 seeds/ μm^2). Growing at an angle from the surface, these truncated prismatic crystals do not display any well-defined order neither in their habit nor in their alignment (Fig. 6b, inset). This leads to an XRD pattern containing diffraction peaks corresponding to both (101) and (002) along with that of (200)/(020). The average growth rate of the truncated crystal grains along the *c*-axis is 0.35 $\mu\text{m}/\text{h}$.

The vertical alignment of the zeolite grains is apparent in the Sil-1 films grown from higher seed concentrations (i.e. 30 and 95 seeds/ μm^2) as shown in the insets of Fig. 6c and d. A time series study

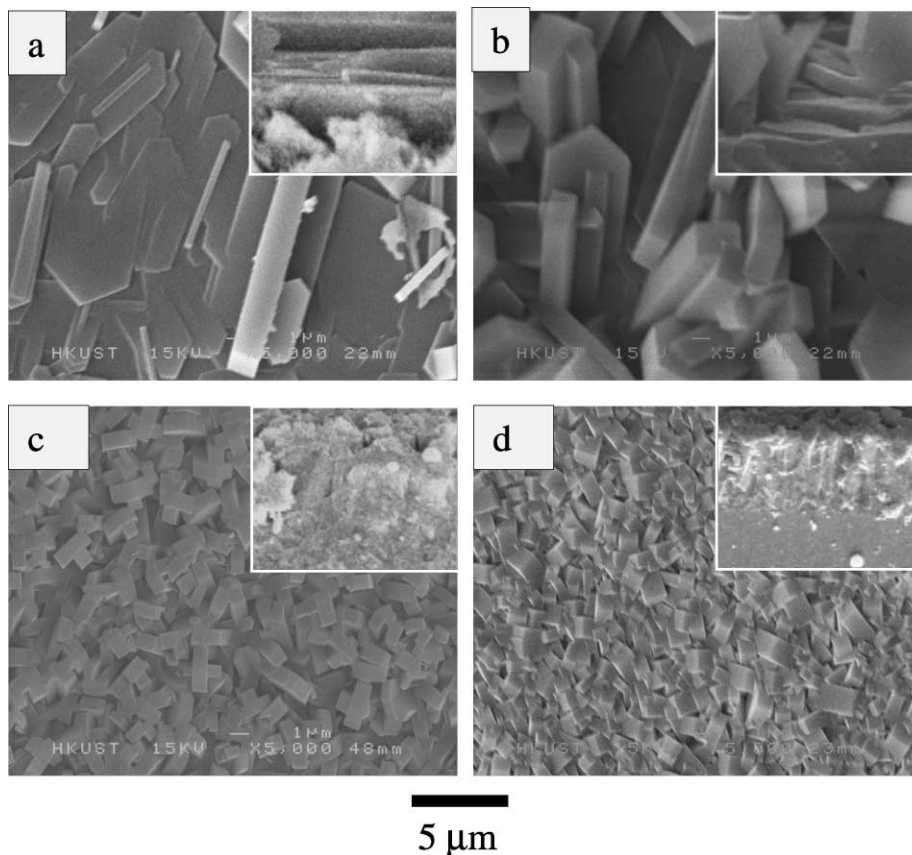


Fig. 6. SEM images of zeolite films grown from the synthesis solution containing $40\text{SiO}_2:9\text{TPAOH}:9500\text{H}_2\text{O}:160\text{EtOH}$ at 448 K for 20 h on silicon pre-seeded with (a) 0, (b) 7.5, (c) 30 and (d) 95 seeds/ μm^2 .

indicated that the individual grains growing from nanometer sized seed crystals exhibit an inverted pyramidal shape, but unlike in Fig. 4e and f the crystals terminated in a prismatic roof instead of a flat plane. This gave the films a rougher surface as shown by the figure insets. Despite their (002)-orientation, the film surface is entirely made up of (101) facets. The growth rates along the *c*-axis for the two samples were estimated from the thickness of the membrane. An average value of $0.25 \mu\text{m}/\text{h}$ was obtained for both samples. Analysis of the film cross-section suggests significant coalescence and intergrowth between competing neighbors, which give rise to a change in grain morphology. A recent modeling work of Bonilla et al. [41] gave a good insight and discussion on the formation of (002)-oriented zeolite membranes from a uni-

formly seeded support prepared from the dilute synthesis solution.

3.2.3. Boric acid synthesis solution (recipe 6)

The spherical shape of the zeolite powder prepared from the boron-containing synthesis solution (recipe 6) is evident from the film shown in Fig. 7a. The hemispherical grains display the same large-radius curvature (Fig. 7a, inset) that characterizes the boron Sil-1 powder (Fig. 2d). Diffraction peaks corresponding to (200)/(020) and (501)/(051) are present in the sample (Fig. 7d-1). Increasing the seed population from 5 to 8 seeds/ μm^2 leads to an intergrown film with a smaller grain size (Fig. 7b) and a smoother surface (Fig. 7b, inset). The XRD pattern in Fig. 7d-2 displays a stronger signal from the high miller index planes (i.e. (501)/

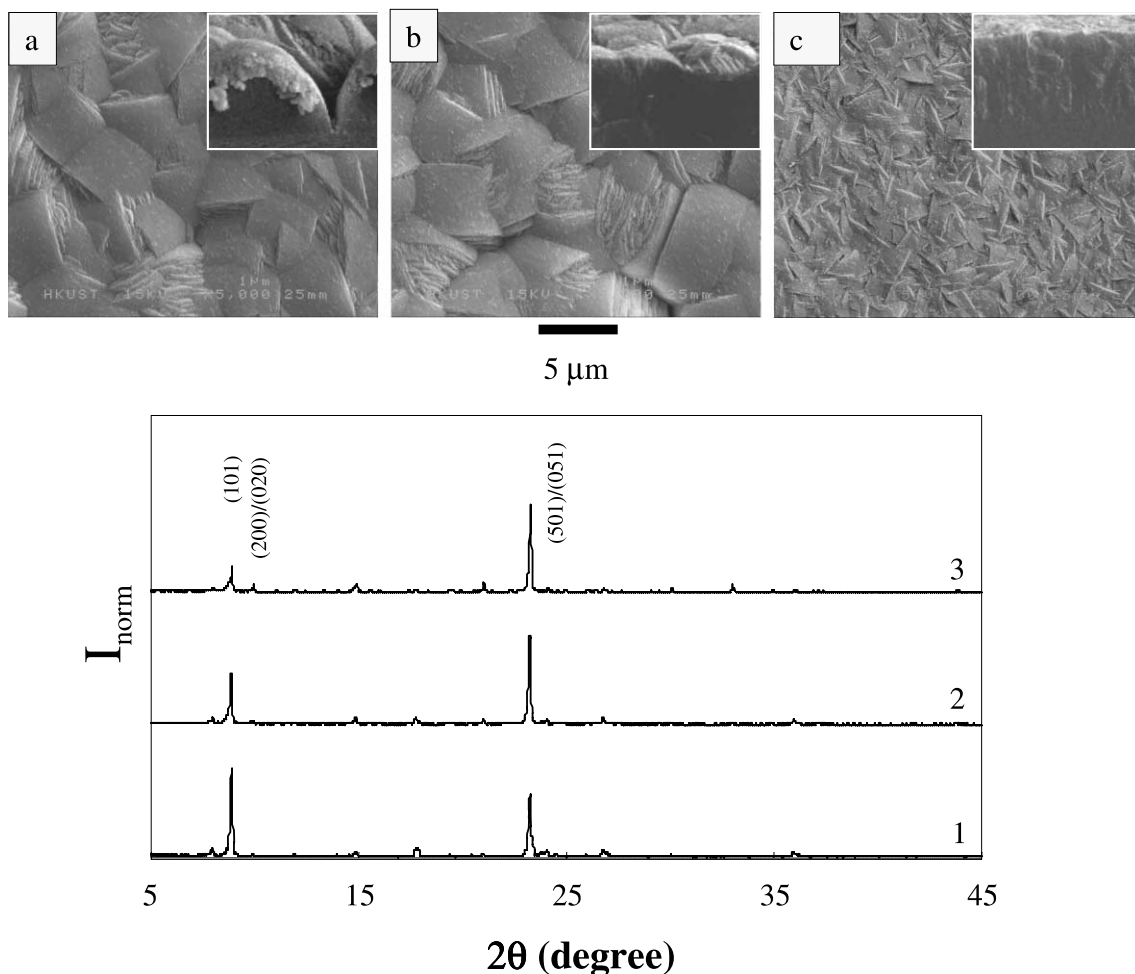


Fig. 7. SEM images of zeolite films grown from synthesis solution containing 40SiO₂:10TPAOH:40 boric acid:20,000H₂O:160EtOH at 403 K for 192 h on silicon pre-seeded with (a) 5, (b) 8 and (c) 95 seeds/μm², and their corresponding X-ray diffraction patterns (1—5, 2—8 and 3—95 seeds/μm²).

(051)). The zeolite layer grown on completely seeded silicon forms a continuous film of highly intergrown grains (Fig. 7c). The film cross-section still exhibits a slight undulation but is significantly flatter than the films prepared at lower seed concentrations (Fig. 7c, inset). It is difficult to distinguish the individual zeolite grains that made up the layer. A stronger (501)/(051) diffraction signal (Fig. 7d-3) indicates a gradual change in film orientation with increasing seed population.

Although a precise mathematical model can be constructed to predict the evolution of the film

microstructure, if the exact zeolite growth kinetics, is given it is always useful to have a simple guide for predicting the film microstructure and orientation from the powder morphology. This will enable the rapid screening of available synthesis recipes and avoid the necessity of obtaining detailed zeolite growth kinetics in advance, which is dependent on the synthesis composition, precursor material, crystallization condition, as well as the presence of impurities. This study demonstrates that the crystal morphology and habit play an important role for the zeolite film microstructure

and orientation. The crystal morphology can be extrapolated from the powder, and its habit can be predicted from the growth vectors. The family of all possible growth vectors emanating from a growth center (e.g. seed) on a flat support should define a hemispherical volume. For less than a monolayer of seeds, the fastest growing axis of the zeolite (i.e. anisotropic growth) should align with one of these growth vectors and *should* not exhibit any preferred habit. However, one should also consider the interfacial surface free energy between the crystal and support. A low interfacial energy means that a large contact area between the support and zeolite is favorable.

The nature of these growth vectors suggests that film orientation can evolve during film growth and this has been observed in a time series study. More importantly it showed that, for a given thickness, bringing the growth centers closer together increases the overlap and decreases the set of favorable growth vectors (i.e. outside an overlapped area). When the volume of the cone defined by these vectors shrinks to zero, a single uniform crystal habit is expected. Using this argument it is possible to explain the effects of seed population on the film microstructure and orientation. It is clear from Figs. 4, 6 and 7, that the zeolite grains retain some of the morphological features of the powder. Recipes 1 and 2 yielded prismatic and twinned powder crystals that have an anisotropic shape. Grown on a flat substrate these zeolites can assume different crystal habits that are mainly constrained by the presence of the support (as illustrated in Fig. 3b). The set of all *possible* growth vectors for the zeolite defines a hemispherical volume with the seed at the center. However, due to a favorable interfacial free energy between silicalite-1 and silicon, the growth vectors that parallel the surface of the substrates are more favored. If the growth centers are brought closer to one another (Fig. 3c), growth competition will result in rapid nutrient depletion in the areas between neighboring grains (see overlapped area in Fig. 3c). A lower mass transfer rate into these confined areas may also play an important role. This means that the growth of the crystals in these areas will be unfavorable. This results in a greater number of off-plane growth that allows the faster growing

c-axis better access to the synthesis solution. The growth vectors within a cone outside the overlapping areas are favored. Under this condition, a polycrystalline zeolite film with random orientation is obtained. At high seed density (Fig. 3d), the most favorable growth vector is normal to the support. This leads to the vertically aligned crystal grains observed in Fig. 4d and e and Fig. 6c and d.

Silicalite-1 crystal powder grown in the presence of boron exhibits a near-spherical shape (Fig. 3e). Ignoring the individual facets, one can assume that the growth of boron silicalite-1 is isotropic and the crystal growth vectors occupy a spherical volume with the seed at the center. On a flat support, the individual boron silicalite-1 grains assume a hemispherical shape, and their growth vectors are defined by a hemispherical volume. The high surface free energy of curved surfaces in boron silicalite-1 grains favors intergrowth (Fig. 3g). Increasing the seed population results in increased growth overlap between neighboring grains and leads to the surface morphology depicted in Fig. 3h. Indeed, the schematic drawings in Fig. 3f–h faithfully reproduce the observed morphology of the boron Sil-1 film shown in Fig. 7a–c. The volume occupied by the growth vectors shrink steadily from a hemisphere to a cone to a single vector pointing outward from the support. The change in growth vectors, as well as the intense growth competition that lead to the coalescence of neighboring crystals are mainly responsible for the pyramidal grains reported for recipes 1 and 2, and the conical grains observed in boron silicalite-1 film.

4. Concluding remarks

This work demonstrates that, besides the synthesis chemistry and crystallization condition, the growth environment also plays a determining role in zeolite film orientation. The local growth environment was manipulated through seeding of the support with zeolite nanoparticles. This study clearly showed that one can obtain different zeolite film microstructures and orientations (i.e. (0 2 0), (2 0 0), random and (1 0 1)) from the same synthesis solution and condition by simply changing the

seed concentration. It is evident from the experimental results that the synthesis composition and crystallization condition have a larger impact on the crystal grain morphology, whereas the crystal habit is mostly dictated by the growth environment. This explains how a single synthesis recipe can lead to zeolite films and membranes of different morphologies and orientations, and why the same film orientation can be prepared from a great variety of synthesis compositions and conditions as reported in both patents and the scientific literature. This work also provides a simple method for predicting the orientation of zeolite films based on the morphology of the zeolite crystal and the growth environment.

Acknowledgements

The authors gratefully acknowledge the funding provided by the Hong Kong Research Grant Council (RGC-HKUST 6072/99P and DA-G00.EG19) and ExxonMobil Chemical Europe Inc. We thank Dr. A.J. Bons and M.H.C. Anthony for their help and suggestions, and we also thank the Materials Characterization and Preparation Facility (MCPF) of the Hong Kong University of Science and Technology (HKUST) for the use of XRD and SEM.

References

- [1] R.M. Barrer, *Hydrothermal Chemistry of Zeolites*, Academic Press, New York, 1982.
- [2] A. Iwasaki, I. Kudo, T. Sano, Real time observation of growth and dissolution of silicalite crystal, in: H. Chon, I.-K. Ihm, Y.S. Uh (Eds.), *Studies in Surface Science and Catalysis*, vol. 105, Elsevier, Amsterdam, 1997, p. 317.
- [3] D.T. Hayhurst, *Zeolites* 8 (1998) 416.
- [4] E.G. Derouane, S. Detremmerie, Z. Gabelica, N. Blom, *Appl. Catal.* 1 (1981) 101.
- [5] F.-Y. Dai, M. Suzuki, H. Takahashi, Y. Saito, *Bull. Chem. Soc. Jpn.* 61 (1988) 3403.
- [6] Z. Gabelica, N. Blom, E.G. Derouane, *Appl. Catal.* 5 (1983) 227.
- [7] J.C. Jansen, C.W.R. Engelen, H. van Bekkum, Crystal growth regulation, in: M.L. Occelli, H.E. Robson (Eds.), *ACS Symposium Series 398*, ACS, Washington, 1989, p. 257.
- [8] G. Perego, G. Bellusi, A. Carati, R. Millini, V. Fattore, Disordered pentasil-type borosilicates, in: M.L. Occelli, H.E. Robson (Eds.), *ACS Symposium Series 398*, ACS, Washington, 1989, p. 360.
- [9] H. Lerner, M. Draeger, J. Steffen, K.K. Unger, *Zeolites* 5 (1985) 131.
- [10] M. Hagiwara, Y. Kiyozumi, M. Kurita, T. Sato, H. Shimada, K. Suzuki, S. Shin, A. Nishijima, S. Todo, *Chem. Lett.* 2 (1981) 1653.
- [11] M. Inaba, H. Hamada, Zeolite synthesis using 1,6-diamino-hexane-based organic diammonium salts as templates, in: I. Kiricsi, G. Pál-Borbély, J.B. Nagy, H.G. Karge (Eds.), *Studies in Surface Science and Catalysis*, vol. 125, Elsevier, Amsterdam, 1999, p. 125.
- [12] T. Sano, S. Sugawara, Y. Kawakami, A. Iwasaki, M. Hirata, I. Kudo, M. Ito, M. Watanabe, In situ observation of crystal growth of silicalite under hydrothermal synthesis condition, in: J. Weitkamp, H.G. Karge, H. Pfeifer, W. Hölderich (Eds.), *Studies in Surface Science and Catalysis*, vol. 84, Elsevier, Amsterdam, 1994, p. 187.
- [13] A. Iwasaki, M. Hirata, I. Kudo, T. Sano, S. Sugawara, M. Ito, M. Watanabe, *Zeolites* 15 (1995) 308.
- [14] A. Iwasaki, M. Hirata, I. Kudo, T. Sano, *Zeolites* 16 (1996) 35.
- [15] A. Iwasaki, T. Sano, *Zeolites* 19 (1997) 41.
- [16] A. Iwasaki, T. Sano, Y. Kiyozumi, *Micropor. Mesopor. Mater.* 25 (1998) 119.
- [17] Z. Gabelica, E.G. Derouane, Synthesis of pentasil zeolites, in: T.E. Whyte, R.A. Dalla Betta, E.G. Derouane, R.T.K. Baker (Eds.), *Catalytic Materials: Relationship Between Structure and Reactivity*, American Chemical Society, Washington, 1983, p. 219.
- [18] J.C. Jansen, The preparation of molecular sieves, in: H. van Bekkum, E.M. Flanigen, J.C. Jansen (Eds.), *Studies in Surface Science and Catalysis*, vol. 58, Elsevier, Amsterdam, 1991, p. 77.
- [19] E.V. Rebrov, G.B.F. Seijger, H.P.A. Calis, M.H.J.M. de Croon, C.M. van den Bleek, J.C. Schouten, in: *Proceedings of the Fourth International Conference on Microreaction Technology*, Atlanta, USA, 2000, p. 250.
- [20] Y.S.S. Wan, J.L.H. Chau, K.L. Yeung, A. Gavriilidis, *Micropor. Mesopor. Mater.* 42 (2001) 157.
- [21] T. Bein, *Chem. Mater.* 8 (1996) 1636.
- [22] S. Feast, J.A. Lercher, Synthesis of intermediates and fine chemicals using molecular sieve catalysts, in: H. Chon, S.I. Woo, S.E. Parks (Eds.), *Studies in Surface Science and Catalysis*, vol. 102, Elsevier, Amsterdam, 1996, p. 363.
- [23] J. Coronas, J. Santamaria, *Separat. Purificat. Meth.* 28 (1999) 127.
- [24] H. Suzuki, Composite membrane having a surface layer of an ultra-thin film of cage-shaped zeolite and processes for production thereof, US Patent no. 4699892, assigned to Suzuki, 1987.
- [25] J.G. Tsikoyiannis, W.O. Haag, *Zeolites* 12 (1992) 126.
- [26] W.O. Haag, J.G. Tsikoyiannis, Separation of mixture components over membrane composed of a pure molecular

- sieves, US Patent no. 5069794, assigned to Mobil Oil Corp., 1991.
- [27] J.C. Jansen, W. Nugroho, H. van Bekkum, Controlled growth of thin films of molecular sieves on various supports, in: R. von Ballmos, J.B. Higgins, M.M.J. Treacy (Eds.), *Proceedings of the Ninth International Zeolite Conference*, Butterworth-Heinemann, Boston, 1993, p. 247.
- [28] E.R. Geuss, H. van Bekkum, W.J.W. Bakker, A. Moulijn, *Micropor. Mater.* 1 (1993) 131.
- [29] M. Noack, P. Kolsch, J. Caro, M. Schneider, P. Toussaint, I. Sieber, *Micropor. Mesopor. Mater.* 35 (2000) 253.
- [30] M.J. den Exter, H. van Bekkum, C.J.M. Rijn, F. Kapteijn, J.A. Moulijn, H. Schellevis, C.I.N. Beenakker, *Zeolites* 19 (1997) 13.
- [31] Y. Yan, S.R. Chaudhuri, A. Sarkar, *Chem. Mater.* 8 (1996) 473.
- [32] K. Aoki, K. Kusakabe, S. Morooka, *J. Memb. Sci.* 141 (1998) 197.
- [33] M.C. Lovallo, M. Tsapatsis, T. Okubo, *Chem. Mater.* 8 (1996) 1579.
- [34] S. Yamazaki, K. Tsutsumi, *Micropor. Mater.* 4 (1995) 205.
- [35] L.C. Boudreau, J.A. Kuck, M. Tsapatsis, *J. Memb. Sci.* 152 (1999) 41.
- [36] A. Kulak, Y.J. Lee, Y.S. Park, K.B. Yoon, *Angew. Chem. Int. Ed.* 5 (2000) 39, 950.
- [37] G. Xomeritakis, A. Gouzinis, S. Nair, T. Okubo, M. He, R.M. Overney, M. Tsapatsis, *Chem. Eng. Sci.* 54 (1999) 3521.
- [38] L.T.Y. Au, K.L. Yeung, *J. Memb. Sci.* 194 (2001) 33.
- [39] J. Hedlund, S. Mintova, J. Sterte, *Micropor. Mesopor. Mater.* 28 (1999) 185.
- [40] Van der Drift, *Philips Res. Rep.* 22 (1967) 267.
- [41] G. Bonilla, D.G. Vlachos, M. Tsapatsis, *Micropor. Mesopor. Mater.* 42 (2001) 191.
- [42] J.P. Verduijn, A.J. Bons, M.H.C. Anthonis, L.R. Czarnetzki, Molecular sieves and processes for their manufacture, WO Patent no. 96/01683, assigned to Exxon Chemical Patents Inc., 1996.
- [43] L.H. Chau, W.C. Wong, K.L. Yeung, in: *Proceedings of the Fifth International Conference on Inorganic Membranes*, Nagoya, Japan, 1998, p. 432.